



Shallow gas high-resolution seismic signatures in a subtropical estuary

João Fernando Pezza Andrade¹ · M. A. Noernberg^{1,2} · R. H. Nagai^{1,2}

Received: 10 December 2020 / Accepted: 3 June 2021 / Published online: 30 July 2021
© The Author(s), under exclusive licence to Springer-Verlag GmbH Germany, part of Springer Nature 2021

Abstract

High-resolution seismic surveys were carried out at the Paranaguá Estuarine Complex (Southern Brazil) to map the intra-sedimentary shallow gas. The seismic signatures representing gas accumulation were separated according to the upper gas boundary characteristics in acoustic blanking with sharp top, acoustic blanking with diffuse top, turbidity pinnacles, and black shadows (gas accumulation at the water/sediment boundary). The main source of the gas has been recognized here as Pre-Holocene continental deposits. These deposits were capped by a seismic unit interpreted as a regressive mud deposited over the last 5000 years. This seismic unit is quite heterogeneous, the gas being trapped in its different internal layers. Each gas signature represents the efficiency of the sealing layer and has specific locations and burial depths. The results point to different phases of gas migration along with the sedimentary layers. Thus, we proposed a gas migration and accumulation model based on acoustic data and sedimentary inferences within the Paranaguá Estuarine Complex.

Introduction

Intra-sedimentary gas accumulation in marine and coastal environments has been recognized in seismic records for decades (Emery and Hoggan 1958; Schubel 1974; Taylor 1992). The presence of shallow gas in seismic data can totally or partially mask the stratigraphical information (Judd and Hovland 1992). Within unconsolidated sediments, gas may accumulate in extensive areas in estuaries and bays (Garcia-Gil et al. 2002; Baltzer et al. 2005; Felix and Mahiques 2013; Delavy et al. 2016a), lagoons (Baltzer et al. 2005; Klein 2005; Weschenfelder and Corrêa 2018), and shallow marine regions (Okyar and Ediger 1999; Missiaen et al. 2002; García-García et al. 2007).

Gas in sediments can derive from biogenic processes, as a product of organic matter microbial decomposition (Rice and Claypool 1981; Gang and Jiang 1985), or thermogenic degradation (Rice and Claypool 1981; Horsfield and Rullkotter 1994). The latter is associated with petroleum generation, mainly developed during the catagenesis and metagenesis stages (Horsfield and Rullkotter 1994; Rooney et al. 1995). In marine

environments, methane (CH₄) is the main gas produced by biogenic decomposition (Claypool and Kaplan 1974; Floodgate and Judd 1992) and during the post-mature metagenesis thermal stage (Horsfield and Rullkotter 1994), which differs from biogenic methane through a heavier methane carbon isotope ratio (Rice and Claypool 1981; Rooney et al. 1995).

The biogenic processes are the primary source of gas accumulation in coastal environments (Lee et al. 2005; García-García et al. 2007; Visnovitz et al. 2015; Vardar and Alpar 2016), normally associated with a shallow basement (Garcia-Gil et al. 2002; Missiaen et al. 2002; Weschenfelder and Corrêa 2018). While thermal gas production needs high temperatures and considerable burial depths (Schoell 1988; Horsfield and Rullkotter 1994; Littke et al. 1999), methanogens microorganisms survive at temperatures between 0 and 75 °C (Zeikus 1977; Gang and Jiang 1985). Biogenic gas production can occur immediately after the sediment deposition in inland water bodies (Gang and Jiang 1985). However, in marine and coastal environments, the presence of sulfate inhibits the production close to the sediment/water boundary, whereas it may occur under the sulfate reduction zone (Nikaido 1977; Rice and Claypool 1981). High rates of CH₄ generation require abundant organic matter, high sedimentation rate, and enough interstitial space for methanogens ($\pm 1 \mu\text{m}$) (Missiaen et al. 2002; García-García et al. 2007). Also, accumulation requires a sealing layer, generally associated with fines and compact sediments (Rogers et al. 2006).

✉ João Fernando Pezza Andrade
jfernando.geof@gmail.com

¹ Coastal and Ocean Systems Graduate Course, Federal University of Paraná, Curitiba, PR, Brazil

² Center for Marine Studies, Federal University of Paraná, Curitiba, PR, Brazil

In the right conditions, the biogenic methane can accumulate in large amounts and is responsible for more than 20% of the world's discovered gas reserves (Rice and Claypool 1981).

Methane is the second most important greenhouse gas after carbon dioxide (CO₂), with 28 times global warming potential over one hundred years (Ciais et al. 2013). Still, there is uncertainty in the estimates of its natural sources and sinks and how its variations can affect the growth rate of atmospheric CH₄ (Borges et al. 2016). Although some studies estimate the CH₄ flux from coastal gas-charged sediments to the atmosphere via immediate water plumes and pockmarks (Judd et al. 1997; Dimitrov 2002; Garcia-Gil et al. 2002), there is insufficient knowledge about methane dynamics within unconsolidated sediments.

Natural gas-charged sediments are recognizable in seismic records by an abrupt decrease of acoustic velocity with possible phase inversion and signal reverberation through bubble resonance (Gorgas et al. 2003; Baltzer et al. 2005). The gas can appear in various shapes and geometries in seismic profiles, classified into distinct gas signatures. The seismic gas signatures are related to different accumulation and seepage types. Their distribution and features can explain the sedimentary structures and their characteristic (Garcia-Gil et al. 2002; Baltzer et al. 2005; García-García et al. 2007).

The present paper aims to map and describe seismic gas signatures in the Paranaguá Estuarine Complex (PEC) and discuss their dynamics linked to the regional stratigraphy. This study suggests a gas migration and accumulation model based on acoustic data. It is important to incorporate information about the gas dynamics within unconsolidated sediments, seismic gas signatures, and stratigraphic meanings. Also, we indicate and discuss the possible source of the shallow gas and the sedimentary unit that acts as a sealing.

Settings

The PEC is a microtidal subtropical estuary system located in the Paraná state, southern Brazil (Fig. 1). The system comprises two main water bodies, Paranaguá Bay and Laranjeiras Bay. The estuarine complex has a 551.8 km² water body surface with 136 km² of tidal flat and 295.5 km² of vegetated flooded areas (Noernberg et al. 2006). The PEC mean depth is 5.4 m, and the maximum depth is around 33 m at the mouth zone (Fig. 1) (Lana et al. 2001). This estuarine system is partially stratified with asymmetric tides (Knoppers et al. 1987). The tidal range is about 2.7 m, and the maximum flood and ebb-tidal current is about 1.2 m/s and 1.4 m/s, respectively (Lamour et al. 2007). The tide intrusion is about 12.5 km (Lana et al. 2001) with a tidal prism of 1.34 km³, and the freshwater flow rate is about 200 m³/s (Lessa et al. 1998).

The estuarine system is embedded in a coastal plain bordered by the Serra do Mar mountain range. The Serra

do Mar mountain range, which reaches over 1500 m (Lana et al. 2001), displays steep slopes and has high erosive potential (Noernberg 2001). West of Paranaguá city, the estuary morphology is characterized as a drowned, narrow, incised paleo-valley (Fig. 1). To the east of Paranaguá city, it comprises a wide coastal plain (Fig. 1). The coastal plain is composed of a sand barrier with at least two generations of beach/dunes ridge progradation, forming a late Pleistocene and a Holocene strand plain (Lessa et al. 2000; Angulo 2004). These sedimentary facies were formed during the two transgressive/regressive cycles related to the last sea-level maximum at Pleistocene and mid- to late-Holocene (Angulo and Suguio 1995; Lessa et al. 2000). Since the last one, the sea level gradually decreased by 3.5 m (Angulo and Lessa 1997).

Continental deposits associated with the Alexandra formation occur in low isolated hills (Angulo 2004) and may comprise, with their reworked material (Bigarella et al. 1978), the substrate for Pleistocene and Holocene sedimentation within the PEC (Lessa et al. 1998, 2000). The Alexandra formation comprises Miocene arkosic sands and muds with lesser gravels and clays (Angulo and Suguio 1995). Sedimentary facies were interpreted as braided channels, dense underwater flows, and gravitational flow deposition, suggesting a depositional system of alluvial fans associated with small aqueous bodies (Angulo 2004). The crystalline basement under the coastal plain is reached at depths of about 50 m landward and about 100 m close to the shoreline (Lessa et al. 2000). Also, gravimetric data investigation along the shoreline indicates a maximum depth of 160 m (Castro et al. 2008). Under the estuarine system, Lessa et al. (1998) suggested a shallower depth of the basement, between 20 to 30 m, corroborated by several small rocky islands within the PEC.

The paper by Lessa et al. (1998) is the only publication about the stratigraphic evolution of the PEC. Using seismic data and several core samples, the authors interpreted four Holocene sedimentary units overlying a pre-Holocene fluvial and continental deposit (Alexandra formation and their reworked material) (Fig. 1). According to the authors, the sea-level rise resulted in a transgressive mud deposit, probably associated with a low-energy estuary funnel environment, followed by transgressive sand. The sand unit overlaid a Tidal Ravinement Surface (Catuneanu 2006), which eroded almost completely the transgressive mud west of Paranaguá. The subsequent highstand system tract includes a regressive mud, which comprises most of the recent superficial sediments in the central zone of the estuary, and regressive sand restricted to the estuary head. Noteworthy, the authors did not mention the presence of gas. However, they recognized non-penetration seismic signal layers, which were tentatively interpreted in different ways.

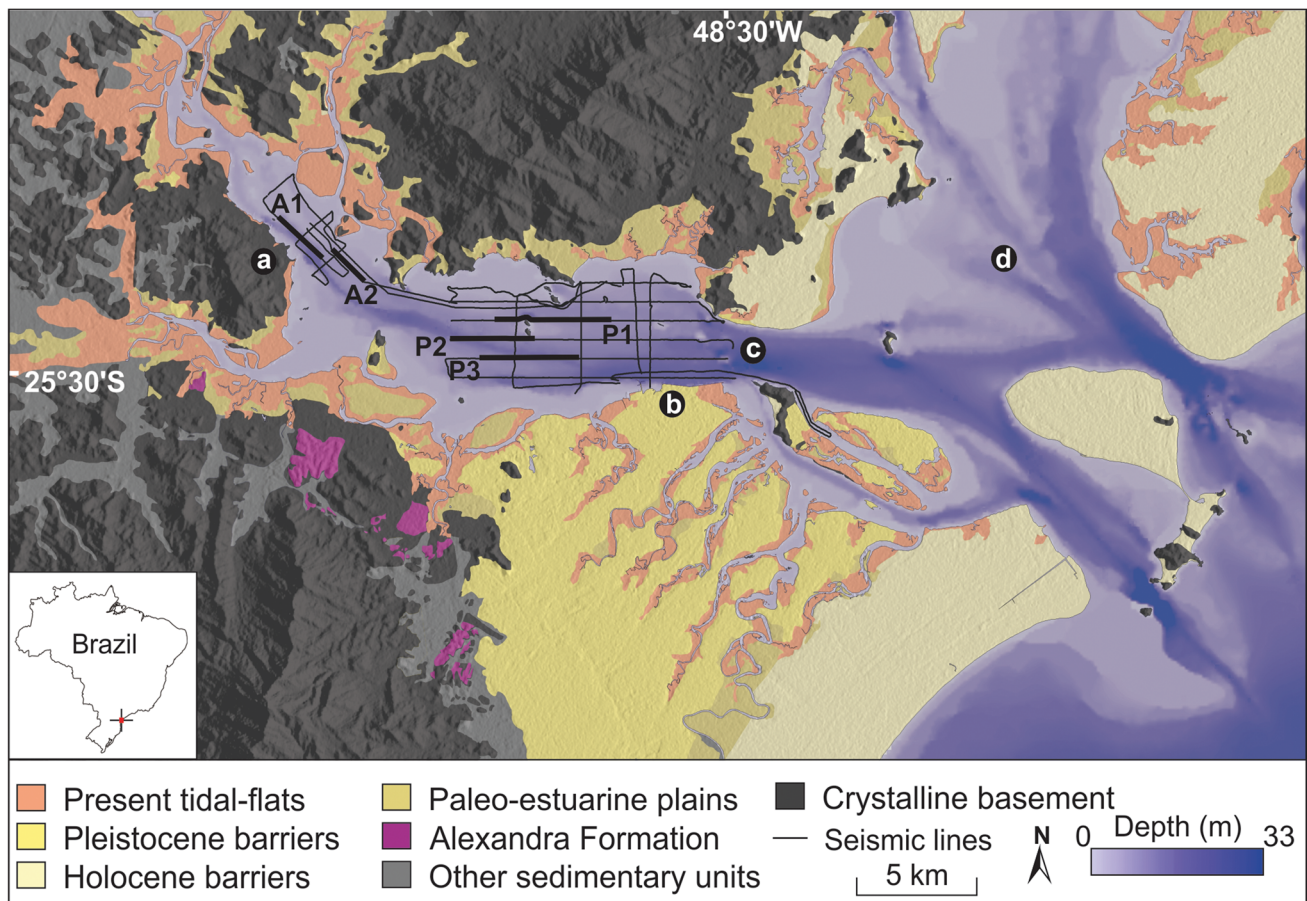


Fig. 1 The Paranaguá Estuarine Complex bathymetric map, and Pleistocene evolution (based on Lessa et al. 2000), with the position of the seismic lines analyzed in this study (P1, P2, P3 in Fig. 4; A1, A2 in Fig. 5). **a** Antonina city; **b** Paranaguá city; **c** Paranaguá Bay; **d** Laranjeiras Bay

Materials and method

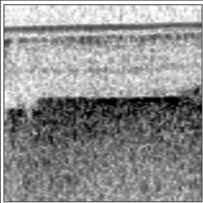
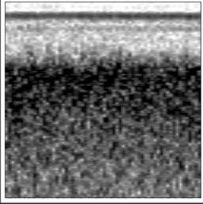
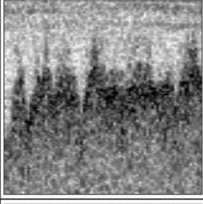
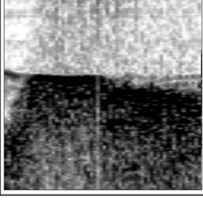
Shallow, high-resolution seismic records were acquired in two PEC zones, using two CHIRP seismic sources (Meridata Finland Ltd) with different frequencies range 2–9 kHz and 10–18 kHz. A total of 156 km of the acquisition was collected over a three-day survey, one in April and two in July 2019 (Fig. 1). Data were processed and interpreted with the Meridata MDPS software. The time to depth conversion was made with a sound velocity of 1500 m/s for both water and sediments; thus, depth in images is approximate. Vertical mean resolution is about seven cm for the lower frequency and three cm for the high frequency. The facies were primarily classified with the lowest frequency of the CHIRP source (Fig. 2) due to its higher penetration in the sediment layers. Although the characterization was done mainly with the 2–9 kHz frequency, the 10–18 kHz CHIRP source was used to assist in the mapping and characterizing the facies and stratification.

Superficial sediment samples were performed with a Van Veen Grab sampler in about fifty PEC locations (Fig. 3).

For grain size analysis, 2 g of sediment was separated from each sample. Afterward, decarbonization was performed with 10% hydrochloric acid (HCl) and the removal of organic matter with 10% hydrogen peroxide (H₂O₂). Grain-size analyses were then performed with a Malvern Mastersizer 2000 through laser diffraction. The data were processed with the Sysgran 3.2 Software (Camargo 2006), later separated by the mud content (silt and clay) (Fig. 3). Because these analyses were initially carried out in another research project, organic matter content data for these samples are not available. However, other studies show that, in the PEC, fine sediments generally have a higher organic matter content (Cattani 2012).

Near distance analyses were performed using the ArcMap software to ascertain the relationship of the bottom sediments with shallow gas (< 1.5 m). Initially, the surface sediment samples acquired with a maximum distance of 200 m from the seismic lines were separated. Then, the distance between these samples and the gas accumulation covered by a sedimentary layer less than 1.5 m was analyzed. The 1.5 m value was picked due to a good statistical correlation

Fig. 2 Intrasedimentary gas seismic signatures observed in the Paranaguá Estuarine Complex classified with a 2–9 kHz CHIRP source and their acoustic characteristic. The scale of all images is 5 m × 100 m

Gas accumulation types		Gas seismic signatures	Description
Acoustic Blanking	Sharp Top (ABS)		High to moderate amplitude with well-defined flat or dipping top. Completely masking the data below.
	Diffuse Top (ABD)		High to moderate amplitude with poorly defined top. Completely masking the data below
Turbidity Pinnacles (TP)			High to moderate amplitude, cone shaped pinnacles with varying dimensions. Generally found as a set with tens of centimeters to a few meters between the pinnacles top and bottom .
Black Shadow (BS)			High amplitude associated with multiples, completely masking the data. Located at the sediment/water boundary, however, it may have portions covered by thin sedimentary layers

between the shallow gas presence and fines content in the Arousa estuary (Diez et al. 2007). Finally, the results were plotted on a graph of distance versus mud content.

Results

At the PEC, the gas signatures found were classified as acoustic blanking (AB) (Judd and Hovland 1992; Lee et al. 2005; Lodolo et al. 2012; Visnovitz et al. 2015; Weschenfelder et al. 2016; Jaśniewicz et al. 2019), black shadow (BS) (Baltzer et al. 2005; Delavy et al. 2016a, b; Felix and Mahiques 2013; Klein et al. 2005; Weschenfelder et al. 2016), and turbidity pinnacles (TP) (Delavy et al. 2016a, b; Felix and Mahiques 2013; Iglesias and García-Gil 2007; Klein et al. 2005; Weschenfelder et al. 2016) (Fig. 2). Together, these gas accumulation facies cover 60 km of the studied area, comprising a total of 38% of the seismic profiles (Fig. 3).

The uppermost portion of the estuary, the Antonina zone, presents a gas signature sector, where the BS facies is on the sides, and the AB facies is frequent in the central portion (Fig. 3). In the Paranaguá zone, gas accumulation is

mainly concentrated in the central region, where the gas accumulation represents different gas seismic facies types along the seismic lines (Fig. 4). However, it is still possible to recognize different gas accumulation sectors in this zone (Fig. 3). The seaward limit of the gas is evident, enabling us to recognize the gas accumulation boundaries in all seismic lines east of the Paranaguá city (Fig. 3).

Acoustic blanking (AB) with sharp (ABS) or diffuse top (ABD)

The AB facies was separated according to the type of reflection at the top, which were either sharp (ABS) or diffuse (ABD) (Fig. 2). ABD facies are the most common in the surveyed area, more than 30 km of total extension, with a maximum continuous extension of 6300 m and a minimum of 15 m (Fig. 3). This facies has a poorly defined top, although it is possible to recognize the gas front (Figs. 4 and 5). It was recognized in water depths ranging from 1.6 m to 16.7 m, with sedimentary coverage between 0.7 m and 6.2 m. This facies covers a large part of the surveyed south and southeast region in the Paranaguá zone and the central and northern regions in the Antonina zone

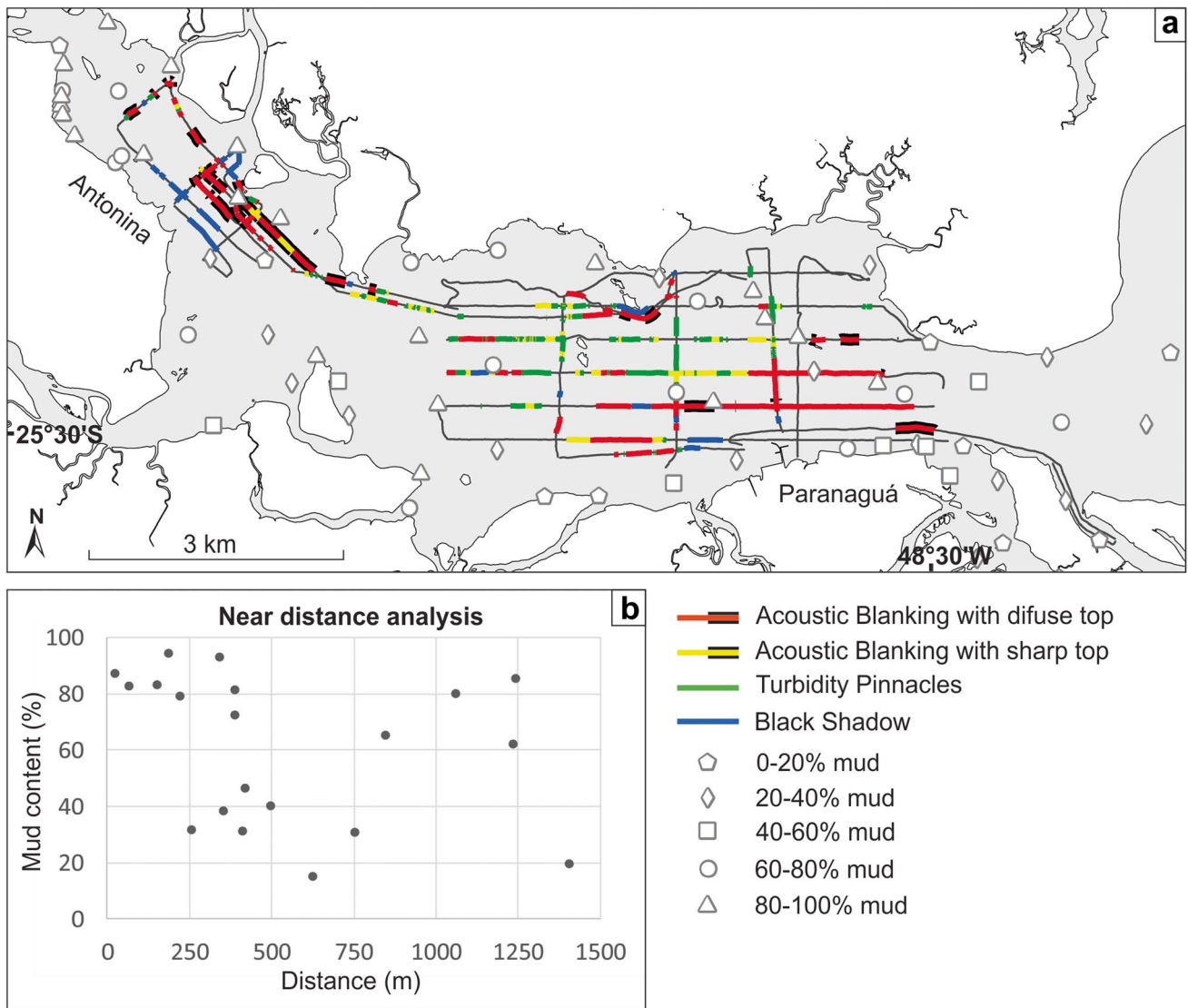


Fig. 3 Location map of the different intrasedimentary gas seismic signatures observed in the Paranaguá Estuarine Complex (seismic data acquisition lines in black) and surficial sediment (0–3 cm) mud content (silt + clay) distributions. Black contour in color lines indicate

gas presence under less than 1.5 m of sediment cover. Near distance analysis graphic represents the closest distance between shallow gas accumulation (<1.5 m), comprising the BS and portions of the ABS and ABD marked by the black contour

(Fig. 3). In the Antonina zone, the gas is shallower, with an average sediment cover of about 1.4 m, while in Paranaguá, the average sediment cover is two times thicker. Also, except for BS, the shallower portion of the gas (< 1.5 m of sedimentary cover) found in the study area is predominantly comprised of the ABD seismic signature (Fig. 3).

ABS facies have a well-defined, flat or inclined top. This facies is characterized by an enhanced reflector that completely masks the data below. ABS facies is frequent in the Paranaguá zone, mainly in the basin center (Fig. 3). It is usually associated with turbidity pinnacles, fitted between the pinnacles (P1 in Fig. 4) or on their lateral limits, and in

conjunction with the ABD facies. This facies covers 8761 m of the seismic profiles, having a minimum extension of 5 m and a maximum of 768 m (Fig. 3). The ABS facies are under 2.2 m to 10.3 m of water and a sediment layer between 0.8 m and 8.5 m with a mean value of 4 m. Like ABD, the ABS is much shallower within the sediments in the Antonina zone than in Paranaguá, with an average difference of more than 4 m sediment cover between them. Also, there are locations where the ABS signatures are shallower in the Antonina zone than 1.5 m in the sedimentary layer.

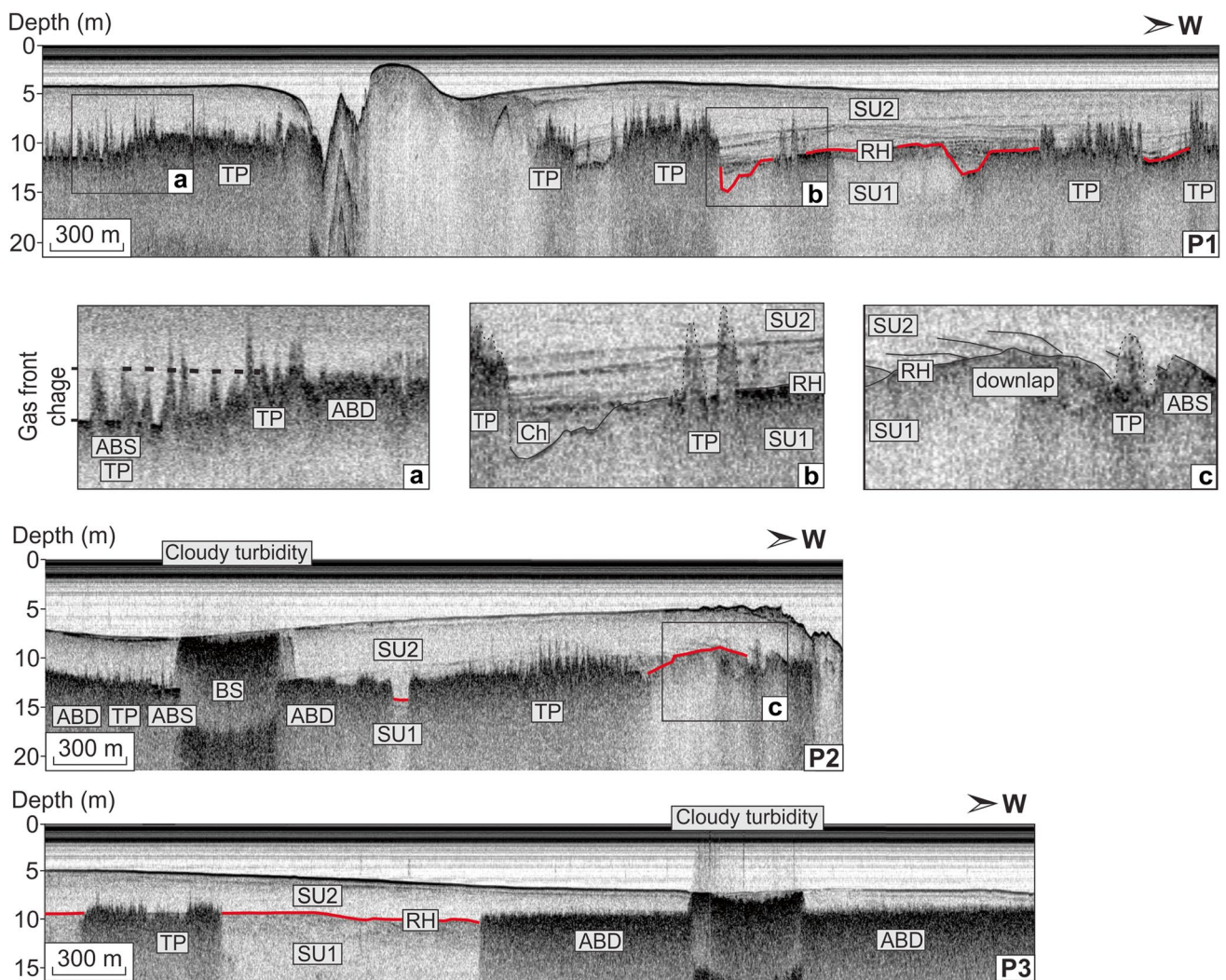
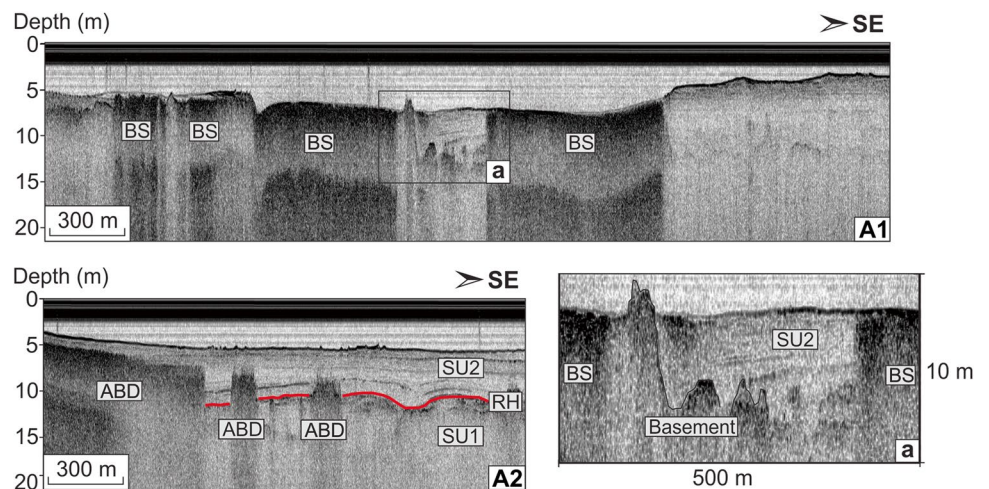


Fig. 4 Chirp (2–9 kHz) seismic profiles in the Paranaguá zone (P1, P2, P3; see Fig. 1 for location) showing gas accumulation seismic signatures (TP, BS, ABS, ABD) and the two seismic units (SU1, SU2) separated by a regional reflector (RH). Detailed zoom images (a, b, c

with 10×500 m scale) indicate a gas accumulation baseline change, paleochannel (Ch), and downlap termination. TP, turbidity pinnacles; BS, black shadow; ABS, acoustic blanking with a sharp top; ABD, acoustic blanking with diffuse top

Fig. 5 Chirp (2–9 kHz) seismic profiles in the Antonina zone (A1, A2; see Fig. 1 for location) showing gas accumulation seismic signatures (BS, ABD) and the two seismic units (SU1, SU2) separated by a regional reflector (RH). Detailed zoom image indicates a stratigraphic window with a shallow basement. BS, black shadow; ABD, acoustic blanking with diffuse top



Turbidity pinnacles (TP)

TP covers about 12 km from the surveyed area. It can be found in isolation or large groups, reaching extensions of almost 1 km (Figs. 3 and 4). TP is often associated with changes in the depth of the gas accumulation, related to the change of the gas sealing layer (Fig. 4a), and may also be between ABS and ABD facies (P2 in Fig. 4). This gas feature is rare in the Antonina zone and concentrated in the Paranaguá zone center (Fig. 3). The TP facies appears in all depths, deeper than 8 m, and reaching the sediment/water limit.

Black shadow (BS)

BS facies cover 8272 m of the seismic profiles, with a maximum length of 1044 m and a minimum of 59 m (Fig. 3). A strong reflector characterizes the BS facies almost in the contact between water and sediment located at depths between 2.3 m and 14.2 m. (Fig. 2). The difference between the BS and ABS types of gas accumulation is that, in the former, it is generally not possible to recognize the sealant sediment layer between the gas accumulation and the water column. The BS sealing layer is less compact than the ABS sealing layer due to the absence of the sediment weight. Additionally, most of the BS facies shows the presence of cloudy turbidity (Garcia-Gil et al. 2002) of lesser or greater intensity (P2 and P3 in Fig. 4), indicating possible seeps to the water column.

The most extensive BS is at the edge of the surveyed area (Fig. 3). In the Paranaguá zone, this facies is usually associated with other gas accumulation types (Fig. 4). On the other hand, in the Antonina zone, the BS facies covers much of the southwest region, appearing in isolation of other gas accumulation types (Fig. 3). In this location, the crystalline basement appears to be shallow (Fig. 5a). Similarly, a BS in the north margin of the Paranaguá zone also presents close to the shallow basement, inferred by the proximity of a rocky island (Fig. 3).

Bottom sediments

Grain size analysis indicates that the PEC bed is predominantly composed of silt with varying amounts of clay and sand. Generally, the mud content decreases towards estuarine margins (Fig. 3). Overall, surveyed regions with subsurface gas present surficial sediment with more than 60% of mud. This pattern has an exception at the north of Paranaguá city, where, above the ABD facies surface, sediments present 30.7% of mud (rhombus symbol north to Paranaguá city in Fig. 3), here the gas is covered by a sediment layer of about 3 m thickness.

The presence of gas shallower than 1.5 m correlates with the sampled sites with the highest concentration of mud, between 80 and 100% (Fig. 3). Graphical analyses also showed that the sample locations closest to gas occurrences shallower than 1.5 m necessarily have a high mud content (Fig. 3b). However, a high concentration of fines does not necessarily indicate the presence of shallow gas (Fig. 3b). Two sampling sites, at the northwest part of the Antonina zone and at the southeastern part of the Paranaguá zone, with more than 80% of mud on seismic lines without subsurface gas were recognized (Fig. 3a), more than 1000 m away from shallow (<1.5 m) gas accumulation (Fig. 3b). There are also two locations, at the southeast of the Paranaguá zone and at the southeast of the Antonina zone, where the samples closer to the gas accumulation have a mud content of less than 40% (Fig. 3). However, there are seismic lines in which the presence of gas has not been recognized (Fig. 3).

Stratigraphy

Although the PEC gas features cover more than a third of the surveyed area, it is possible to recognize some stratigraphic characteristics. A regional horizon (RH) is recognized in most stratigraphic windows (P1 in Fig. 4 and A2 in Fig. 5). This horizon represents an irregular relief with numerous paleochannels (P1 in Fig. 4).

The RH separates two distinct seismic units. The older unit (SU1) has no distinguishable reflectors (Fig. 4), or in some places, reflectors with a chaotic pattern (Fig. 5). Above this horizon, the seismic unit (SU2) presents flat or slightly wavy internal reflectors. In the distal portion of the Paranaguá zone, the internal reflectors of SU2 show progradation over RH (Fig. 4c). In the Antonina zone, there are places with the absence of SU1 where it is possible to observe direct contact of the basement with the SU2 unit (Fig. 5a). No tectonic structure, such as faults or folds, has been recognized in the acoustic data.

Discussion

High-resolution seismic gas signatures

Four types of seismic gas signatures were observed at the PEC, with unique spatial distribution and depth. In the coastal plain adjacent to the study area, drill-holes reached the crystalline basement at depths of about 50 m (Lessa et al. 2000). This shallow depth of the basement is hindering the possibility of thermogenic gas generation within the sedimentary section (Rice and Claypool 1981). Thus, even though this study did not perform a chemical analysis of the gas (i.e., isotopic measurements), it is highly probable

that PEC gas-charged sediments result from organic matter degradation by biogenic activity.

There are several terminologies for the different seismic signatures caused by gas accumulation. However, these terminologies are often confusing, having several names for similar seismic signatures, or even the opposite, the same names for different seismic signatures (Weschenfelder et al. 2016). For example, despite the consensus to separate gas accumulation signatures in acoustic blankets and acoustic curtains through their format and lateral extension (Taylor 1992; Garcia-Gil et al. 2002; Klein et al. 2005; Vardar and Alpar 2016), there is a discrepancy as to the type of the top of the gas occurrence. Acoustic curtains are smaller, with a concave shape, while the blankets are flatter and cover large areas. However, some works indicate that acoustic curtains have a main top reflector and blankets have a diffuse top, without the presence of a strong reflector (Taylor 1992), or conversely, where the curtain has a less sharp upper gas boundary (Garcia-Gil et al. 2002; Frazão and Vital 2007). More usually, works indicate that both have a high amplitude reflector at the top (Baltzer et al. 2005; Vardar and Alpar 2016; Weschenfelder et al. 2016).

The separation of the curtain and blanket facies was not used here, as this separation does not seem to imply different properties from the type of gas accumulation, such as gas quantity by volume or a different permeability of the sealing layer. These properties are better related to the upper boundary seismic signature of gas accumulations (Taylor 1992; Garcia-Gil et al. 2002). The facies extensions are best seen through maps (as Fig. 3) and the different shapes of the gas curtain—box (Weschenfelder et al. 2016; Weschenfelder and Corrêa 2018), Chevron (Garcia-Gil et al. 2002; Frazão and Vital 2007), convex (Garcia-Gil et al. 2002), or mushroom (Karisiddaiah et al. 1993). This feature characterizes either the sealing layer topography or of the lateral decrease in seismic wave speed caused by the gas (Garcia-Gil et al. 2002), which can also occur on the sides of the acoustic blanket and other gas accumulation types (“pull-down”; Judd and Hovland 1992; Lee et al. 2005; Vardar and Alpar 2016).

Gas accumulation types were classified here mainly in terms of their top, in sharp (ABS), diffuse (ABD), and highly diffuse (TP). Black shadows were also separated for their unique characteristics. Each seismic signature represents a specific feature of the gas accumulations in the sediments. The different seismic signatures and their depths and locations provide information on the stages of migration and accumulation of shallow gas in the PEC (Fig. 6), discussed later in this paper (“Shallow gas migration and accumulation within unconsolidated sediments in PEC” section). It is worth to highlight that the seismic signatures found in this work refer to the presence of shallow intrasedimentary gas observed in a shallow bay. This gas is trapped by

a Holocene sedimentary unit with a high content of fines and imaged by CHIRP type acoustic source (2–9 kHz and 10–18 kHz). Therefore, the seismic signatures associated with gas accumulation from different coastal environments with other environmental parameters (water depth, gas depth, sediment background) or acquired with other seismic sources can vary considerably from those presented here.

Acoustic blanking (AB) with sharp (ABS) or diffuse top (ABD)

We interpret the difference between ABS and ABD gas accumulation type due to the efficiency of the sealing layer. This efficiency is represented by the permeability contrast of the source and sealing layer (Garcia-Gil et al. 2002) and gas (Taylor 1992). The results showed that ABS facies is, on average, at greater buried depths. This aspect highlights the importance of pressure for forming this facies, as greater depths accentuate sediment compaction, decreasing the permeability of the sealing layer (Nooraiepour et al. 2019). The sealing layer can retain the gas for a longer time, increasing the gas concentrations. The amount of gas can increase up to a limit, after which gas seeps into the low permeability sealing layer, generating pinnacles (Figs. 4a and 6d). This aspect explains the almost absence of ABS facies at the Antonina zone and its presence at the Paranaguá zone center, where gas is observed in greater depths. Also, sealing layer efficiency in the Antonina zone should be lower due to a minor mud content caused by the tapered morphology and the fluvial influence. Despite this difference, both ABS and ABD facies portray high gas accumulation, sufficient to mask the acoustic data (> 30 ml/L; Whelan et al. 1977).

Additionally, at the PEC, ABS facies are smaller and less common than ABD facies (Fig. 3). This indicates that the lowest permeability layers are rarer to form and do not reach large extensions, probably due to the heterogeneity of compaction (possible sediment reworking or bioturbation) and grain-size (similar to the existing surface of the estuary).

Turbidity pinnacles (TP)

TP facies indicate an upward migration of the gas without an efficient and relatively homogeneous sealing layer. Due to this characteristic, TP can be found at any depth in the sedimentary strata. The heads of TP facies may eventually find a low permeability layer, where the gas will accumulate (Fig. 6b and e) until the forming of acoustic blanking facies (Figs. 4a and 6). When associated with ABS facies, TP may indicate a rupture in the sealing layer (Figs. 4a and 6d). In contrast, when associated with ABD facies, a less common association in the study area, TP must indicate a differentiated gas migration, probably associated with the difference in the amount of gas or heterogeneities of the sealing layer. When close to the sediment–water interface,

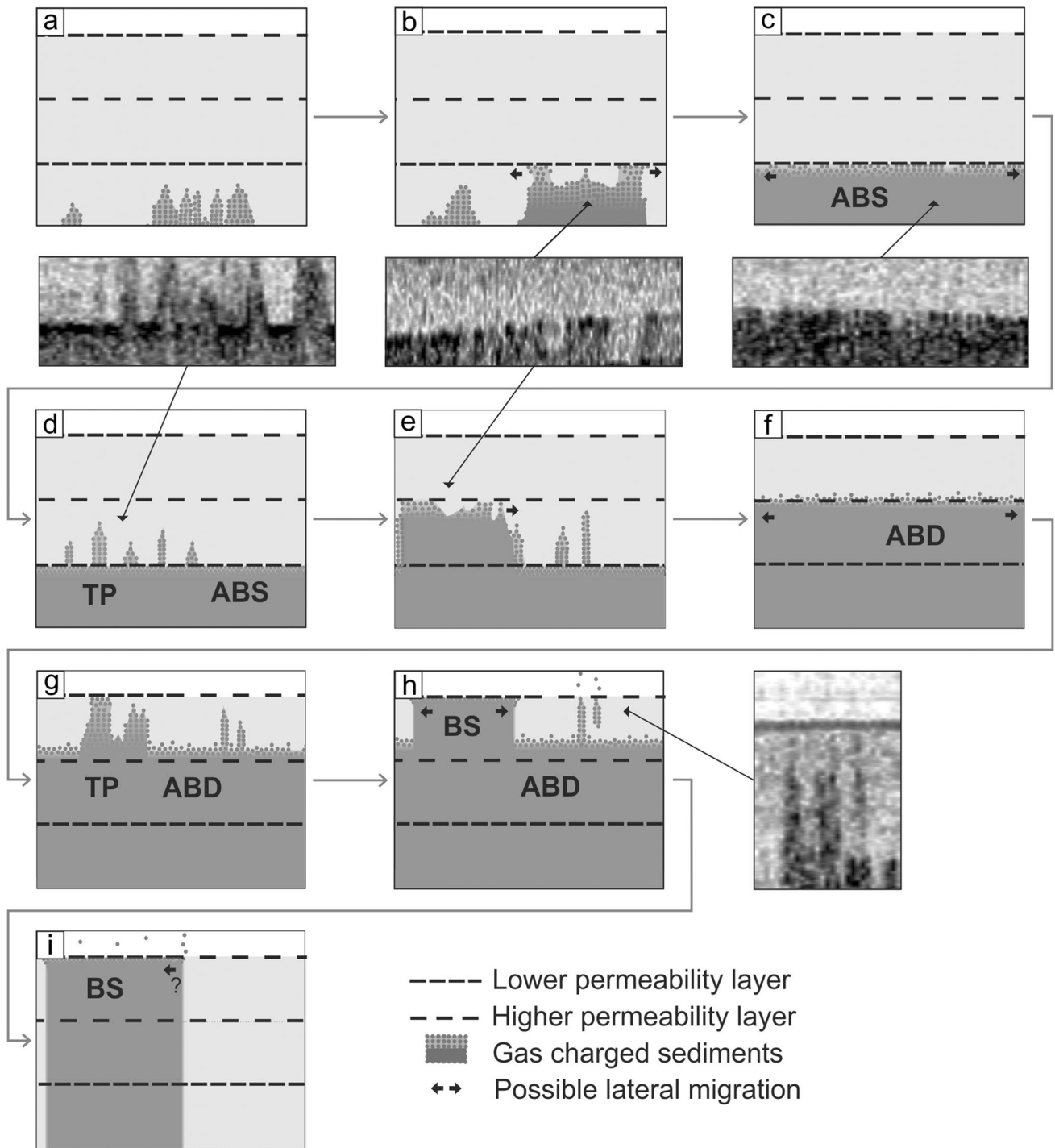


Fig. 6 Evolution model of shallow gas migration and accumulation, showing the changes between seismic gas signatures and their relationship with the relative permeability between sedimentary layers. The gas migrates from the source as turbidity pinnacles (a); the pinnacles head encounter a low permeability layer and start to accumulate (b); the gas accumulates forming an acoustic blanking with a sharp top (c); eventually, the gas seeps to the low permeability layer forming pinnacles (d); again the heads of pinnacles encounter a sealing layer, and de gas start to accumulate (e); this time the sealing

layer has low trapping efficiency and thus the gas slowly seeps when it accumulates forming an acoustic blanking with diffuse top signature (f); heterogeneities in the sealing layer permits turbidity pinnacles locally formation (g); the pinnacles reach the sediment–water interface and can accumulate as a black shadow or seeps to the water column (h); finally, the gas slowly seeps from the black shadow to the water column (i). Note that the model above has only two sedimentary layers for didactic means. In the PEC, the amount of layers capable of retaining the gas, and their relative permeability, varies locally

the TP gas front can be trapped, forming BS gas accumulation type or, supposedly, the gas should seep into the water column (Fig. 6h).

Most TP facies were found in the Paranaguá zone center, being scarce in Antonina (Fig. 3). In the latter, gas accumulation occurs at shallower depths, and, thus, gas accumulation must be portrayed as other gas seismic signatures closest to the surface or reached the water column (Fig. 6h). This pattern is explained by the lower efficiency of the sealing layer in Antonina.

Black shadow (BS)

The BS facies represents the last stage of gas trapping within unconsolidated sediments (Fig. 6). The close to the surface in situ gas production hypothesis (Baltzer et al. 2005) does not apply here due to the influence of sulfate-rich seawater (Nikaido 1977; Rice and Claypool 1981; Gang and Jiang 1985). However, we cannot exclude the possibility of gas generation locally near the lower limit of the sulfide reduction zone, which can migrate to the sediment–water boundary.

Noteworthy, the BS facies were located even at small depths, little more than 2 m. Therefore, the hydraulic pressure is not a limiting factor for the formation of the BS. Also, it is impossible to observe the thickness of the sealant sediment layer, implying that this layer is very thin or, more likely, being passed through. Thus, we argue that grain-size must be the main factor that allows or hampers the creation of BS, not being able to have significant bioturbation or reworking of the superficial sediments. The dependence on grain-size may explain the maximum BS facies size observed in this work. Worth noting that there is substantial heterogeneity in the bottom sediments (Fig. 3).

In PEC, regions where the basement is shallow, gas accumulates as BS, and no other gas seismic signature is observed. We suggest that these regions have a thinner seal layer or layers, so it is easier for the gas to migrate upward and concentrate at the sediment/water boundary. If the BS facies does not have an active gas source, it should disappear over time due to the gas seepage to the water column. In this sense, BS facies are probably not stable seismic signatures. In the Paranaguá zone, where BS facies is associated with other facies, it may be increasingly charged with gas from below. In the Antonina zone, upward gas migration must be at an advanced stage (Fig. 6g), probably due to a thinner seal layer.

Shallow gas migration and accumulation within unconsolidated sediments in PEC

The gas migration and accumulation processes are dependent on the gas concentration, pressure gradient, and porosity of the surroundings, which controls the gas migration velocity (Zhou et al. 2018). Due to the strong sedimentary heterogeneity in the PEC, at least in the Holocene unit west of Paranaguá city (Lessa et al. 1998), the estuary is a great natural laboratory to observe different gas migration features, which these driving forces are locally variable. Also, there is no evidence of neotectonics or faults in the sedimentary layers in the PEC region. In the absence of a significant impermeable structural trap, the gas generated within PEC unconsolidated and mostly flat sediment layers should be in constant and slow movement by diffusion and advection. Therefore, the types of gas signatures found at different depths may indicate phases of migration and gas accumulation from its source to the water column associated with differential sedimentary properties.

The CH₄ seepage to the water column and eventually to the atmosphere is little known, as the current works are restricted to recognizing gas plumes in the water column or pockmarks (Judd et al. 1997; Dimitrov 2002; Garcia-Gil et al. 2002). Borges et al. (2016) reported high CH₄ concentrations in surface waters of the Belgian coastal zone associated with the presence of shallow gas in sediments. However, in that region, no plumes or pockmarks were recognized, but noises were reported in the water column close to the seabed (Missiaen et al. 2002). Similarly, noises were recognized in the PEC, mainly above BS. These noises may indicate a methane gas seepage, a minor version of the cloudy turbidity recognized in the water column (P2 and P3 in Fig. 4) (Garcia-Gil et al. 2002).

Along these lines, we propose a migration and accumulation model from the source to the water column of shallow gas in the PEC (Fig. 6), which might apply to other coastal environments. Worth to note, that this is a preliminary model given the current lack of additional data, such as sedimentary column physical properties and composition, which could provide different pathways and forms of gas migration. First, the gas seeps from the source layer, migrating upward in the form of pinnacles (Fig. 6a). Eventually, this gas encounters layers with low permeability that trap the gas. When the pinnacles “head” encounters these layers, the gas begins to accumulate (Fig. 6b, e) and starts to present an acoustic blanking seismic signature. Depending on the trapping efficiency of the sealing layer, the gas is completely trapped, generating an ABS signature (Fig. 6c), or it can slowly escape into the sealing layer as it accumulates, forming an ABD signature (Fig. 6f). In the PEC, the layers with the greatest trapping efficiency are found in greater depth, but the sequence of the layers may vary locally, also the

quantity of sealing layers. In both cases, the gas accumulating below the sealing layer can present lateral migration, causing an abrupt lateral limit (Fig. 6b, c, e, f). When the gas is effectively trapped (ABS), it accumulates to a limit when local “breaks” occur in the sealing layer, again forming pinacles (Fig. 6d), which can also be formed in less efficient sealing layers (Fig. 6g). Finally, when the gas reaches the sediment–water interface, it can be exhumed to the water column or accumulate one last time, forming the BS (h), where the gas should eventually leak (Fig. 6i). A small amount of upper sedimentary layers in situ local gas production cannot be ruled out. However, it should follow the same migration and accumulation patterns mentioned above.

The gas occurring in the PEC sediments consists of biogenic methane. However, it is impossible to differentiate and quantify the current in situ production and the deep gas migration. Thus, through the current PEC data, the temporal variation of the gas contained in the sediments and its seepage to the water column is unknown. Continuous acoustic surveys should be employed to observe temporal or seasonal variations of the gas accumulation in sediments to recognize the gas dynamics’ time scale and the influence of its in situ production. Analyses of the methane concentration in the sediments and water would also be relevant for the possible quantification of the PEC methane contribution to the atmosphere. This would contribute to more robust estimatives of gas seepage in estuarine and coastal environments, currently underestimated (Borges et al. 2016).

Bottom sediments

The PEC bottom sediments are heterogeneous concerning mud content (Fig. 3), probably due to the presence of several distributary channels (Fig. 1). West of Paranaguá city, bottom sediments are associated with the top of the regressive mud (Lessa et al. 1998). Sediment core analyses indicate that the fines content of the regressive mud ranges from 30 to 91%, and the organic matter content ranges from 2.2% to 20% (Lessa et al. 1998), indicating that sedimentary heterogeneity seen in the bottom sediments is also present in all SU2. In PEC, bottom sediments with a high content of fines are related to a higher organic matter content (Cattani 2012). There is no gas accumulation downstream of the Paranaguá zone, where sandy bottom sediments (Lamour et al. 2004) are associated with a transgressive sand layer (Lessa et al. 1998).

Some studies showed that shallow gas accumulation in bays could be related to the mud content of bottom sediments (Garcia-Gil et al. 2002; Diez et al. 2007; Jensen and Bennike 2009). In the PEC, the presence of gas shallower than 1.5 m seems to have a strong correlation with a high mud content in surficial sediments (Fig. 3). On the other hand, samples with a high mud content in the PEC do not

necessarily indicate the presence of gas (Fig. 3b). This observation reinforces the idea that the presence of mud close to the bottom decreases permeability and traps gas from below and does not consist of a gas source.

The occurrence of the BS facies is dependent on a low permeability (Fig. 6h). Thus, it is related to the bottom sediments’ mud and sand contents (Merckelbach and Kranenburg 2004; Nooraiepour et al. 2019). The sample with low mud content close to the BS (rhombus symbol south of Antonina zone in Fig. 3) may indicate that the bottom sand content increase defines the southern limit of this facies.

We state that gas below 1.5 m of sediment does not correlate with the bottom sediments due to the variation of the sedimentary facies in depth. Although samples over the region with a gas presence generally have greater than 60% mud content, there are very few sampling sites in this region. The high mud content in the center of the basin is correlated with the Holocene regressive mud and not necessarily with gas presence in the subsurface.

Stratigraphy

The gas accumulated in marine and coastal environments interspersed in sediments causes a significant effect on the geoacoustic signature (Weschenfelder et al. 2016). In this study, over one-third of the acoustic data obtained in the PEC was covered by gas-associated features. Still, we recognized two very distinct seismic units (SU1 and SU2) separated by an RH reflector. The RH shows several paleochannels and high amplitude.

The older pre-Holocene unit (SU1) is here interpreted as continental deposits formed during low sea-level conditions (Fig. 7), the Alexandra Formation (Angulo 1995; Lessa et al. 1998). This formation has high mud contents and is characterized by deposits interpreted as debris flows (matrix-supported conglomerates), mudflows, or even small swamps (Angulo 1995, 2004). The characteristics of the chaotic seismic pattern recognized in this unit can be associated with debris flows, which have large sparse blocks observed in the Alexandra Formation portion (Angulo 1995, 2004). Similarly, the transparent seismic pattern can be associated with mudflows (muds and sandy muds). However, this study does not include wells to confirm these assumptions. This unit represents the main source of gas, at least in the Paranaguá zone, where it is possible to observe the TP coming out of this unit (P1 in Fig. 4). Also, the RH reflector in the vicinity of TPs that appear to leave SU1 has a greater amplitude than gas-free regions (P1 in Fig. 4), indicating a possible enhanced reflection related to discrete gas accumulation that usually occurs in the edges of more evident gas accumulations (Iglesias and García-Gil 2007; Judd and Hovland 1992). However, we cannot discard the hypothesis of a small amount of gas generation in some mud layers of the SU2.

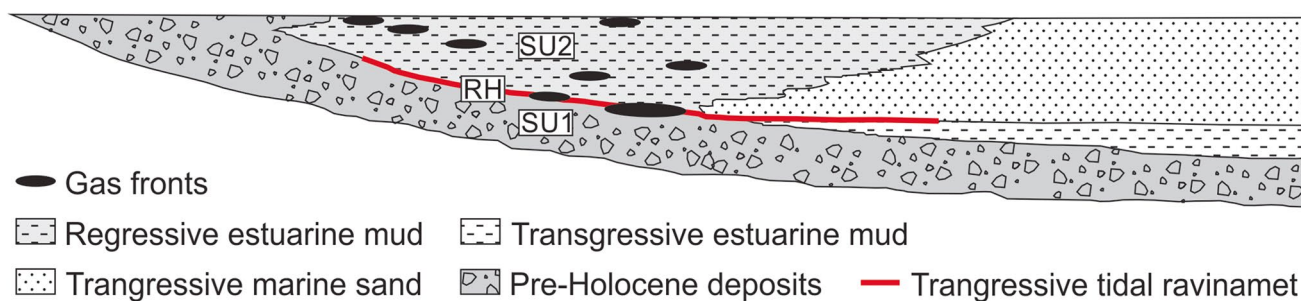


Fig. 7 PEC sedimentary facies evolution (based on Lessa et al. 1998) and the gas-charged sediments recognized in this work

The younger unit (SU2) represents a prograding sedimentary body. Considering Lessa et al. (1998) work, this unit should represent Holocene regressive muds deposited over the last 5000 years (Fig. 7). These authors recognized this unit directly with continental deposits or with a sandy layer associated with transgressive marine sand (Fig. 7). According to Lessa et al. (1998), the contact between these two facies results from a transgressive tidal ravine and tidal diastem associated with the estuary tapering (Fig. 7). We believe that the HR reflector represents this erosion surface (Fig. 7) with tidal channels (Fig. 4b). The SU2 unit is highly heterogeneous, seen through the bottom sediment samples (Fig. 3) and previous studies (Lessa et al. 1998). Changes in bottom water currents due to freshwater outflow and climatic oscillations, or other oceanographic forcings over the past millennia, have resulted in layers with different physical properties (internal reflectors in SU2 Figs. 4 and 5). These layers, observed in SU2, are responsible for trapping the biogenic-derived gas (Fig. 7). The gas slowly migrates within the SU2 (TP), accumulating in the lower permeability layers (ABD and ABS), until it reaches the sediment–water interface, where, if the right conditions exist, the gas may be trapped one last time (BS) (Fig. 6). At the same time, gas trapping by SU2 is corroborated by the absence of gas east of Paranaguá city, where regressive muds are absent (Fig. 7) (Lessa et al. 1998). Also, in some SU2 mud layers rich in organic matter, a small amount of gas can be generated, following the same migration pattern and accumulation mentioned above.

In the Antonina zone, the gas is trapped closer to the sediment–water interface. This shallower gas may be due to a smaller sealing efficiency in internal sedimentary SU2 layers or in situ generation of gas close to the water column. A smaller water depth and a thin SU2 unit in this region generate low gravitational pressure. With less pressure, the efficiency of the sealing layer decreases, and the gas is more easily saturated in sediment porewater (Abegg and Anderson 1997; Lee et al. 2005). Also, the Antonina zone probably has lower efficient sealing layers due to the different environmental settings. This zone has greater fluvial

influence, where coarser sediments derived directly from the fluvial course are deposited, increasing its permeability (Nooraiepour et al. 2019). Another explanation is that the gas source in the Antonina zone is shallower, associated with SU2 muddy layers deposited when the sea level was at its maximum at the mid-Holocene (Angulo et al. 2006). The crystalline basement appears to be shallower in the Antonina zone, and it is possible to see the contact between the SU2 unit and the basement (Fig. 5a). However, possibly the SU1 unit was preserved in the basement troughs, which is not visible in seismic due to the gas presence. Other studies indicated that the source of shallow gas is associated with pre-Holocene units preserved in paleo-valleys (Judd et al. 1997; Garcia-Gil et al. 2002; Weschenfelder et al. 2016). The basement locations close to the gas accumulation (A1 in Fig. 5) may indicate lateral migration (Fig. 6h).

Conclusion

High-resolution seismic surveys were carried out at the Paranaguá Estuarine Complex to analyze intrasedimentary gas accumulation and seismic signatures. The seismic signatures were separated into acoustic blanking with a diffuse top (ABD) or sharp top (ABS), turbidity pinnacles (TP), and black shadow (BS). These features represent distinct gas accumulation types associated with the efficiency of the sealing layer relative to the permeability and gas concentration. As the gas is in constant and slow migration in unconsolidated, mostly flat, sediments layers, seismic gas signatures in the PEC are unstable. Hence, a model of gas migration and accumulation, and its seismic signatures is proposed for the PEC (Fig. 6).

In PEC, the main gas source is associated with the pre-Holocene continental deposits of SU1 unit. While Holocene regressive muds, unit SU2, trap the gas and may have some local layers generating small amounts of biogenic gas. This unit is highly heterogeneous with layers of low permeability that trap the gas at different levels.

Although we cannot determine the gas migration time scale, this work indicates intrasedimentary shallow gas dynamics in coastal environments. We suggest that future work may include continuous seismic surveys to monitor gas accumulation types within sediments and the evaluations of CH₄ in the water column, which would improve our understanding of gas dynamics and gas seepage from coastal environments, and help to unravel the role of estuarine biological methane production on our planet's climate.

Funding The authors would like to thank the Brazilian National Council for Scientific and Technological Development (CNPq) for the financial support through the project “Historical overview and future perspectives regarding the occurrence of chemical stressors present in the Paranaguá Estuarine Complex” approved in Edital MCTIC/CNPq 21/2017 (process n° 441265/2017-0). Thanks are also due to the Brazilian Coordination for Improvement of Higher Education (CAPES) for the research grants and to the Center for Marine Studies of the Federal University of Paraná for the infrastructure.

References

- Abegg F, Anderson AL (1997) The acoustic turbid layer in muddy sediments of Eckernförde Bay, Western Baltic: methane concentration, saturation and bubble characteristics. *Mar Geol* 137:137–147. [https://doi.org/10.1016/S0025-3227\(96\)00084-9](https://doi.org/10.1016/S0025-3227(96)00084-9)
- Angulo RJ (1995) Caracterização e reavaliação da Formação Alexandra (Terciário) e de sedimentos continentais associados a vertentes no litoral do Estado do Paraná, Brasil. *Anais Acad Bras Ciên* 67:445–463
- Angulo RJ (2004) Mapa do Cenozóico do Litoral do Paraná. *Bol Parana Geociências* 55:25–42
- Angulo RJ, Lessa GC (1997) The Brazilian sea-level curves: a critical review with emphasis on the curves from the Paranaguá and Cananeia regions. *Mar Geol* 140:141–166. [https://doi.org/10.1016/S0025-3227\(97\)00015-7](https://doi.org/10.1016/S0025-3227(97)00015-7)
- Angulo RJ, Suguio K (1995) Re-evaluation of the Holocene sea-level maxima for the State of Paraná, Brazil. *Palaeogeography, Palaeoclimatology, Palaeoecology* 113:385–393. [https://doi.org/10.1016/0031-0182\(95\)00055-Q](https://doi.org/10.1016/0031-0182(95)00055-Q)
- Angulo RJ, Lessa GC, De SMC (2006) A critical review of mid- to late-Holocene sea-level fluctuations on the eastern Brazilian coastline. *Quat Sci Rev* 25:486–506. <https://doi.org/10.1016/j.quascirev.2005.03.008>
- Baltzer A, Tessier B, Nouzé H et al (2005) Seistec seismic profiles: a tool to differentiate gas signatures. *Mar Geophys Res* 26:235–245. <https://doi.org/10.1007/s11001-005-3721-x>
- Bigarella JJ, Becker RD, Matos DJ, Werner A (1978) A Serra do Mar e a porção oriental do Estado do Paraná...um problema de segurança ambiental e nacional. Curitiba
- Borges AV, Champenois W, Gypens N et al (2016) Massive marine methane emissions from near-shore shallow coastal areas. *Sci Rep* 6:2–9. <https://doi.org/10.1038/srep27908>
- De CMG (2006) Sysgran: um sistema de código aberto para análises granulométricas do sedimento. *Rev Bras Geociências* 36:371–378
- Camargo MG (2006) Sysgran: um sistema de código aberto para análises granulométricas do sedimento. *Rev Bras Geociências* 36:371–378. <https://doi.org/10.25249/0375-7536.2006362371378>
- Castro LG, Ferreira FJF, Angulo RJ (2008) Modelo gravimétrico-magnético do gráben de paranaguá-PR. *Brasil* 26:273–292
- Cattani PE (2012) Caracterização geomorfológica e sedimentológica do Eixo E-W do complexo estuarino de Paranaguá. Universidade Federal do Paraná
- Catuneanu O (2006) Principles of sequence stratigraphy, 1st edn. Elsevier, Amsterdam, pp 375
- Claypool GE, Kaplan IR (1974) The origin and distribution of methane in marine sediments. In: Kaplan IR (ed) Natural gases in marine sediments. Plenum Press, New York, pp 99–139
- Ciais P, Sabine C, Bala G et al (2013) Carbon and other biogeochemical cycles. In: Stocker et. al. TF (ed) Climate change 2013: the physical science basis. Contribution of Working Group I to the Fifth Assessment Report of the Intergovernmental Panel on Climate Change. Cambridge University Press, Cambridge, pp 104
- Delavy FP, Figueiredo AG, Abuchacra RC et al (2016a) Mapping of gas charged sediments in Guanabara Bay: seismic characteristics and sediment properties. 2015 IEEE/OES Acoust Underw Geosci Symp RIO Acoust 2015. <https://doi.org/10.1109/RIOAcoustics.2015.7473640>
- Delavy FP, de Figueiredo AG Jr, Martins MVA et al (2016b) High-resolution acoustic mapping of gas charged sediments and living benthic foraminifera assemblages from the Ne region of the Guanabara Bay (Rj, Brazil). *J Sediment Environ* 1:360–384. <https://doi.org/10.12957/jse.2016.26281>
- Diez R, García-Gil S, Durán R, Vilas F (2007) Gas accumulations and their association with particle size distribution patterns in the Ría de Arousa seabed (Galicia, NW Spain): an application of discriminant analysis. *Geo-Marine Lett* 27:89–102. <https://doi.org/10.1007/s00367-007-0064-4>
- Dimitrov L (2002) Contribution to atmospheric methane by natural seepages on the Bulgarian continental shelf. *Cont Shelf Res* 22:2429–2442. [https://doi.org/10.1016/S0278-4343\(02\)00055-9](https://doi.org/10.1016/S0278-4343(02)00055-9)
- Emery KO, Hoggan D (1958) Gases in marine sediments. *Am Assoc Pet Geol Bull* 42:2174–2188
- Felix CA, Mahiques MM (2013) Late quaternary evolution and shallow gas formation in a tropical estuarine environment: the case of the Bertioga channel, Brazil. 2013 IEEE/OES Acoust Underw Geosci Symp RIO. <https://doi.org/10.1109/RIOAcoustics.2013.6684003>
- Floodgate GD, Judd AG (1992) The origins of shallow gas. *Cont Shelf Res* 12:1145–1156. [https://doi.org/10.1016/0278-4343\(92\)90075-U](https://doi.org/10.1016/0278-4343(92)90075-U)
- Frazão E, Vital H (2007) Estruturas rasas de gás em sedimentos no estuário Potengi (nordeste do Brasil). *Rev Bras Geofísica* 25:17–26
- Gang ZY, Jiang CH (1985) Concepts on the generation and accumulation of biogenic gas. *J Pet Geol* 8:405–422. <https://doi.org/10.1111/j.1747-5457.1985.tb00281.x>
- García-García A, Orange DL, Miserocchi S et al (2007) What controls the distribution of shallow gas in the Western Adriatic Sea? *Cont Shelf Res* 27:359–374. <https://doi.org/10.1016/j.csr.2006.11.003>
- García-Gil S, Vilas F, García-García A (2002) Shallow gas features in incised-valley fills (Ría de Vigo, NW Spain): a case study. *Cont Shelf Res* 22:2303–2315. [https://doi.org/10.1016/S0278-4343\(02\)00057-2](https://doi.org/10.1016/S0278-4343(02)00057-2)
- Gorgas TJ, Kim GY, Park SC et al (2003) Evidence for gassy sediments on the inner shelf of SE Korea from geoacoustic properties. *Cont Shelf Res* 23:821–834. [https://doi.org/10.1016/S0278-4343\(03\)00026-8](https://doi.org/10.1016/S0278-4343(03)00026-8)
- Horsfield B, Rullkötter J (1994) Diagenesis, catagenesis, and metagenesis of organic matter. *Pet Syst - from source to trap* 189–199. https://doi.org/10.1007/978-3-642-96446-6_6
- Iglesias J, García-gil S (2007) High-resolution mapping of shallow gas accumulations and gas seeps in San Simón Bay (Ria de Vigo, NW Spain). Some quantitative data, pp 103–114. <https://doi.org/10.1007/s00367-007-0065-3>
- Jaśniewicz D, Klusek Z, Brodecka-Goluch A, Bolatek J (2019) Acoustic investigations of shallow gas in the southern Baltic Sea (Polish Exclusive Economic Zone): a review. *Geo-Marine Lett* 39:1–17. <https://doi.org/10.1007/s00367-018-0555-5>
- Jensen JB, Bennike O (2009) Geological setting as background for methane distribution in Holocene mud deposits, Århus Bay,

- Denmark. *Cont Shelf Res* 29:775–784. <https://doi.org/10.1016/j.csr.2008.08.007>
- Judd AG, Hovland M (1992) The evidence of shallow gas in marine sediments. *Cont Shelf Res* 12:1081–1095. [https://doi.org/10.1016/0278-4343\(92\)90070-Z](https://doi.org/10.1016/0278-4343(92)90070-Z)
- Judd A, Davies G, Wilson J et al (1997) Erratum: Contributions to atmospheric methane by natural seepages on the U.K. continental shelf (*Marine Geology* (1997) 137 165–189) PII: S0025322796000874). *Mar Geol* 140:427–455. [https://doi.org/10.1016/S0025-3227\(97\)00067-4](https://doi.org/10.1016/S0025-3227(97)00067-4)
- Karisiddaiah SM, Veerayya M, Vora KH, Wagle BG (1993) Gas-charged sediments on the inner continental shelf off western India. *Mar Geol* 110:143–152. [https://doi.org/10.1016/0025-3227\(93\)90110-H](https://doi.org/10.1016/0025-3227(93)90110-H)
- Klein AH da F, Demarco LFW, Guesser V et al (2005) Shallow gas seismic structures: forms and distribution on Santa Catarina Island, Southern Brazil. *Braz J Oceanogr* 64:157–160
- Knoppers BA, Brandini FP, Thamm CA (1987) Ecological studies in the bay of Paranaguá. II. Some physical and chemical characteristics. *Nerítica* 2:1987
- Lamour M, Soares CR, Carrilho J (2004) Mapas De Parâmetros Texturais De Sedimentos De Fundo Do Complexo Estuarino De Paranaguá – Pr Textural Parameters Maps of Bottom Sediments on Paranaguá Bay Complex – Pr. 77–82
- Lamour MR, Angulo RJ, Soares CR (2007) Bathymetrical evolution of critical shoaling sectors on Galheta Channel, navigable access to Paranaguá Bay, Brazil. *J Coast Res* 231:49–58. <https://doi.org/10.2112/03-0063.1>
- Lana PC, Marone E, Lopes RM (2001) The Subtropical Estuarine Complex of Paranaguá Bay, Brazil. *Ecol Stud* 144:131–145
- Lee GH, Kim DC, Kim HJ et al (2005) Shallow gas in the central part of the Korea Strait shelf mud off the southeastern coast of Korea. *Cont Shelf Res* 25:2036–2052. <https://doi.org/10.1016/j.csr.2005.08.008>
- Lessa GC, Marone E, Meyers SR (1998) Holocene stratigraphy in the Paranaguá Bay estuary, Southern Brazil. *J Sediment Res* 68:1060–1076. <https://doi.org/10.1306/D426890A-2B26-11D7-8648000102C1865D>
- Lessa GC, Angulo RJ, Giannini PC, Araújo AD (2000) Stratigraphy and Holocene evolution of a regressive barrier in south Brazil. *Mar Geol* 165:87–108. [https://doi.org/10.1016/S0025-3227\(99\)00130-9](https://doi.org/10.1016/S0025-3227(99)00130-9)
- Littke R, Cramer B, Gerling P et al (1999) Gas generation and accumulation in the West Siberian basin. *Am Assoc Pet Geol Bull* 83:1642–1665. <https://doi.org/10.1306/e4fd4233-1732-11d7-8645000102c1865d>
- Lodolo E, Baradello L, Darbo A et al (2012) Occurrence of shallow gas in the easternmost Lago Fagnano (Tierra del Fuego). *Near Surf Geophys* 10:161–169. <https://doi.org/10.3997/1873-0604.2011040>
- Merckelbach LM, Kranenburg C (2004) Determining effective stress and permeability equations for soft mud from simple laboratory experiments. *Géotechnique* 54:581–591. <https://doi.org/10.1680/geot.54.9.581.56940>
- Missiaen T, Murphy S, Loncke L, Henriët JP (2002) Very high-resolution seismic mapping of shallow gas in the Belgian coastal zone. *Cont Shelf Res* 22:2291–2301. [https://doi.org/10.1016/S0278-4343\(02\)00056-0](https://doi.org/10.1016/S0278-4343(02)00056-0)
- Nikaido M (1977) On the relation between methane production and sulfate reduction in bottom muds containing sea water sulfate. *Geochem J* 11:199–206. <https://doi.org/10.2343/geochemj.11.199>
- Noernberg MA (2001) Processos orofodinâmicos no complexo estuarino de Paranaguá-Pr, Brasil: Um Estudo a Partir De Dados “in Situ” E Landsat-Tm. Universidade Federal do Paraná
- Noernberg M, Lautert L, Araújo A et al (2006) Remote sensing and GIS integration for modelling the Paranaguá estuarine complex-Brazil. *J Coast Res* 1627–1631. <http://www.jstor.org/stable/25743033>
- Nooraiepour M, Mondol NH, Hellevang H (2019) Permeability and physical properties of semi-compacted fine-grained sediments—a laboratory study to constrain mudstone compaction trends. *Mar Pet Geol* 102:590–603. <https://doi.org/10.1016/j.marpetgeo.2019.01.019>
- Okyar M, Ediger V (1999) Seismic evidence of shallow gas in the sediment on the shelf off Trabzon, southeastern Black Sea. *Cont Shelf Res* 19:575–587. [https://doi.org/10.1016/S0278-4343\(98\)00111-3](https://doi.org/10.1016/S0278-4343(98)00111-3)
- Rice DD, Claypool GE (1981) Generation, accumulation, and resource potential of biogenic gas. *Am Assoc Pet Geol Bull* 65:5–25. <https://doi.org/10.1306/2f919765-16ce-11d7-864500102c1865d>
- Rogers JN, Kelley JT, Belknap DF et al (2006) Shallow-water pockmark formation in temperate estuaries: a consideration of origins in the western gulf of Maine with special focus on Belfast Bay. *Mar Geol* 225:45–62. <https://doi.org/10.1016/j.margeo.2005.07.011>
- Rooney MA, Claypool GE, Moses Chung H (1995) Modeling thermogenic gas generation using carbon isotope ratios of natural gas hydrocarbons. *Chem Geol* 126:219–232. [https://doi.org/10.1016/0009-2541\(95\)00119-0](https://doi.org/10.1016/0009-2541(95)00119-0)
- Schoell M (1988) Multiple origins of methane in the Earth. *Chem Geol* 71:1–10. [https://doi.org/10.1016/0009-2541\(88\)90101-5](https://doi.org/10.1016/0009-2541(88)90101-5)
- Schubel JR (1974) Gas bubbles and the acoustically impene-trable, or turbid, character of some estuarine sediments. In: Kaplan IR (ed) *Marine science*. Plenum Press, New York, pp 275–298
- Taylor DI (1992) Nearshore shallow gas around the U.K. coast. *Cont Shelf Res* 12:1135–1144. [https://doi.org/10.1016/0278-4343\(92\)90074-T](https://doi.org/10.1016/0278-4343(92)90074-T)
- Vardar D, Alpar B (2016) High-resolution seismic characterization of shallow gas accumulations in the southern shelf of Marmara Sea, Turkey. *Acta Geophys* 64:589–609. <https://doi.org/10.1515/acgeo-2015-0059>
- Visnovitz F, Bodnár T, Tóth Z et al (2015) Seismic expressions of shallow gas in the lacustrine deposits of Lake Balaton, Hungary. *Near Surf Geophys* 13:433–446. <https://doi.org/10.3997/1873-0604.2015026>
- Weschenfelder J, Corrêa ICS (2018) Shallow gas features and distribution in the patos lagoon: a coastal trap for gas-generator sediments. *Pesqui em Geociencias*, pp 45. <https://doi.org/10.22456/1807-9806.91385>
- Weschenfelder J, Klein AHF, Green AN et al (2016) The control of palaeo-topography in the preservation of shallow gas accumulation: examples from Brazil, Argentina and South Africa. *Estuar Coast Shelf Sci* 172:93–107. <https://doi.org/10.1016/j.ecss.2016.02.005>
- Whelan T, Coleman JM, Suhayda JN, Roberts HH (1977) Acoustical penetration and shear strength in gas-charged sediment. *Mar Geotechnol* 2:147–159. <https://doi.org/10.1080/10641197709379776>
- Zeikus JG (1977) The biology of methanogenic bacteria. *Bacteriol Rev* 41:514–541. <https://doi.org/10.1128/mmb.41.2.514-541.1977>
- Zhou Y, Wojtanowicz AK, Li X et al (2018) Improved model for gas migration velocity of stagnant non-Newtonian fluids in annulus. *J Pet Sci Eng* 168:190–200. <https://doi.org/10.1016/j.petrol.2018.05.025>

Publisher's note Springer Nature remains neutral with regard to jurisdictional claims in published maps and institutional affiliations.